

## GEMS, hydrated chondritic IDPs, CI-matrix material: Sources of water in 81P/comet Wild 2

Frans J. M. RIETMEIJER \*

Earth and Planetary Sciences, University of New Mexico, MSC03-2040, Albuquerque, New Mexico 87131-0001, USA

\*Corresponding author. E-mail: fransjmr@unm.edu

(Received 24 October 2017; revision accepted 01 September 2018)

---

**Abstract**—So far there is no conclusive evidence for water in the nucleus of 81P/comet Wild 2. Recently magnetite in collected Wild 2 samples was cited as proxy evidence for parent body aqueous alteration in this comet (Hicks et al. 2017). A potential source for water of hydration would be layer silicates but unfortunately there is no record, neither texturally nor chemically, for hydrated layer silicates that survived hypervelocity impact in the Wild 2 samples. This paper reports large vesicles in the matrix of allocation C2044,2,41,2,5 from a volatile-rich type B/C Stardust track. These vesicles were probably caused by boiling water that were generated when hydrated Wild 2 silicates impacted the near-surface silica aerogel layer. Potential water sources were partially and fully hydrated GEMS (glass with embedded metal and sulfides) and CI carbonaceous chondrite materials among the earliest dusts that experienced hydration and icy-body formation and long-range transport and mixing with materials from across the solar system.

---

### INTRODUCTION

Spherical objects ranging from ~50 nm to ~1000 nm in size (Rietmeijer 1993), with complex non-chondritic compositional gradients (Joswiak et al. 1996), in an amorphous ferromagnesian silica matrix speckled with Fe-Ni-S nanograins are the defining characteristic of chondritic porous (CP) interplanetary dust particles (IDPs). These unique spherical grains were assigned a bewildering array of names such as “ultrafine-grained” (ufg) principal components (PCs) with a ferromagnesian silica matrix and embedded electron-opaque nanograins (Rietmeijer 1998, 2002). The term GEMS (glass with embedded metal and sulfides) was introduced by Bradley (1994a) who claimed that GEMS were “chemically anomalous, pre-accretionally irradiated grains,” but there is no evidence that all GEMS grains in CP IDPs are presolar grains. The uncertainty about GEMS origins became urgent when interpreting the Stardust minerals (Rietmeijer 2009a, 2009b). The GEMS-like objects in Stardust are probably the results of mixing [Mg-Fe-Si-O] and [Fe-Ni-S] melts (Rietmeijer 2015) but this process cannot explain the presence of GEMS in the

matrix of CP IDPs. The STARDUST mission to Jupiter-Family (J-F) comet 81P/Wild 2 (hereafter Wild 2) (Brownlee et al. 2006) did not provide compelling evidence for GEMS (Zolensky et al. 2006) aside from rare, round glassy objects superficially resembling GEMS in the bulbous part of Type B and Type C tracks (Joswiak et al. 2012; Leroux and Jacob 2013; Rietmeijer 2015, 2016a). Isotopically anomalous presolar GEMS are in fact but a fraction (1–6%) of GEMS in anhydrous chondritic IDPs, that is, the vast majority of GEMS have a solar system origin (Keller and Messenger 2011). It was argued that Wild 2 GEMS would probably not survive hypervelocity (6.1 km s<sup>-1</sup>) capture (Chi et al. 2007) but no impact process is 100% efficient.

It was suggested that GEMS initially formed as mixtures of vapor-condensed magnesian silica and ferrosilica nanoparticles in the early solar system (Rietmeijer 2011). These amorphous nanograins became the stock for numerous <100 nm amorphous ferromagnesian silica grains (Rietmeijer et al. 2013; Rietmeijer and Nuth 2015). Still missing in this mix are metal and sulfide grains. Stoichiometric troilite was the first, and possibly predominant, sulfur-containing mineral that formed on

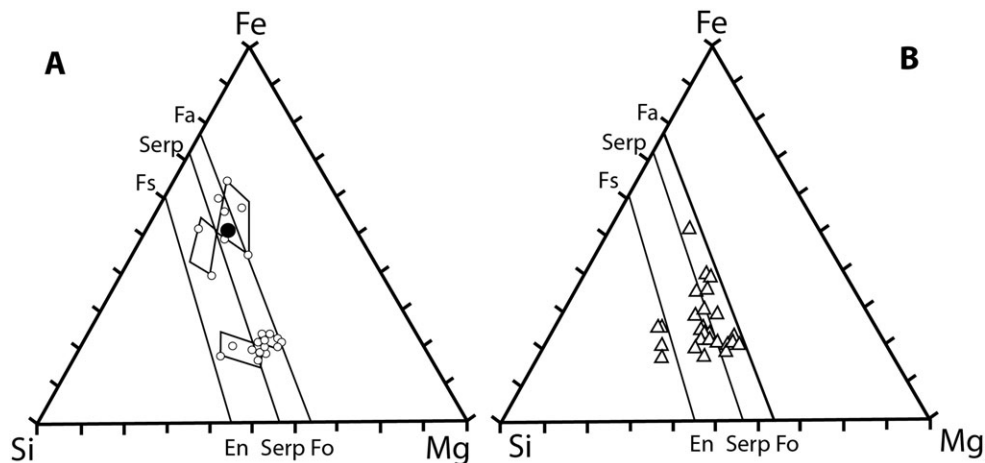


Fig. 1. Mg-Fe-Si diagrams showing the GEMS endmember compositions in two partially hydrated CP IDP L2011K7. The “butterflies” highlight the extents of internal GEMS Mg-Fe-Si variations (Fig. 1a) and the range of individual GEMS bulk compositions in this IDP (Fig. 1b) (Rietmeijer 1996).

Fe-metal grains in the solar nebula, while pyrrhotite grew from sulfidation of exfoliated FeS grains (Zolensky and Thomas 1995). The resulting mix of these amorphous ferromagnesian silicates and sulfides resulted in the GEMS that formed the matrix of CP IDPs in the early solar system (Rietmeijer et al. 2013). Some GEMS fused together; others were hydrated such as those in the matrix of partially hydrated CP IDP L2011K7. Its matrix developed bundles of serpentine and smectite proto-phyllsilicates during aqueous alteration of GEMS (Rietmeijer 2011).

Individual GEMS compositions in the partially hydrated CP IDP L2011K7 range between  $\text{Fe}/(\text{Fe} + \text{Mg}) = 0.30\text{--}0.65$  with internal heterogeneous distributions of Ni and S and, when present, low Al and Ca (Rietmeijer 1998, 2002). GEMS heterogeneity is highlighted by two “butterflies” each showing the extent of Mg-Fe-Si variations (Fig. 1A). The average GEMS compositions in this partially hydrated CP IDP are delimited between the olivine and pyroxene solid solution compositions (Fig. 1B).

The Mg-Fe-Si compositions of very fine-grained Alais and Orgueil matrix material show a narrow band in the Alais meteorite matrix (Fig. 2A) and a similarly trending, but more scattered, band in the Orgueil meteorite matrix (Fig. 2B) (Mackinnon and Kaser 1988). The Si/Fe ratios are highly variable at constant Mg/(Fe+Si) ratios albeit much more scattered in the very fine-grained Orgueil matrix. But, coarser matrix compositions in the Tonk, Alais, Orgueil, and Ivuna CI chondrite meteorites (McSween 1987) have a much more organized Mg-Fe-Si cluster-like distribution (Fig. 2C). The partially hydrated CP IDP L2011K7 compositions (Fig. 1A) resemble the CI-matrix compositions (Fig. 2C). The very fine-grained, low-Mg

Fe-Si, compositions of Alais and Orgueil matrix (Figs. 2A and 2B) resemble some of the GEMS survey compositions (Fig. 3).

This benchmark survey of GEMS compositions (Keller and Messenger 2011) is the starting point to my argument on processing of the oldest and smallest dust in the early solar system such as the partially hydrated GEMS in CP IDP L2011K7 compositions (Rietmeijer 1996) matching the GEMS survey. This survey also includes many Si- and Fe-rich GEMS (Fig. 3; triangle) that resemble the compositions of “equilibrated” aggregates with enclosed metal (Bradley 1994b) and “equilibrated” aggregates (Bradley et al. 1989). These aggregates might be thermally evolved GEMS. The  $\text{Mg}/(\text{Mg} \pm \text{Fe}) = 0\text{--}30$  compositions (Fig. 3; open arrow) resemble those of coarse-grained, low-Mg silica glasses with associated Fe-sulfide grains in chondritic aggregate IDPs (Rietmeijer 1998). They are probably melted and differentiated GEMS clusters (Rietmeijer 2002). The overlapping Mg-Fe-Si compositions of CI chondrite matrices (Fig. 2) and the GEMS survey (Keller and Messenger 2011), including Si-rich GEMS, are quite remarkable and cannot be coincidental. In fact, IR spectroscopy identified serpentine-rich and smectite-rich IDPs (Sandford and Walker 1985) with potential links to carbonaceous chondrites (Tomeoka and Buseck 1985).

I submit the thesis that CI chondrite matrix is an aggregation of fully hydrated GEMS. As no naturally occurring process will be 100% efficient, there will be partially dehydrated GEMS, i.e., such as CP IDP L2011K7, among infrared layer-lattice silicate IDPs (Sandford and Walker 1985). The raw materials for GEMS in the solar nebula were amply available

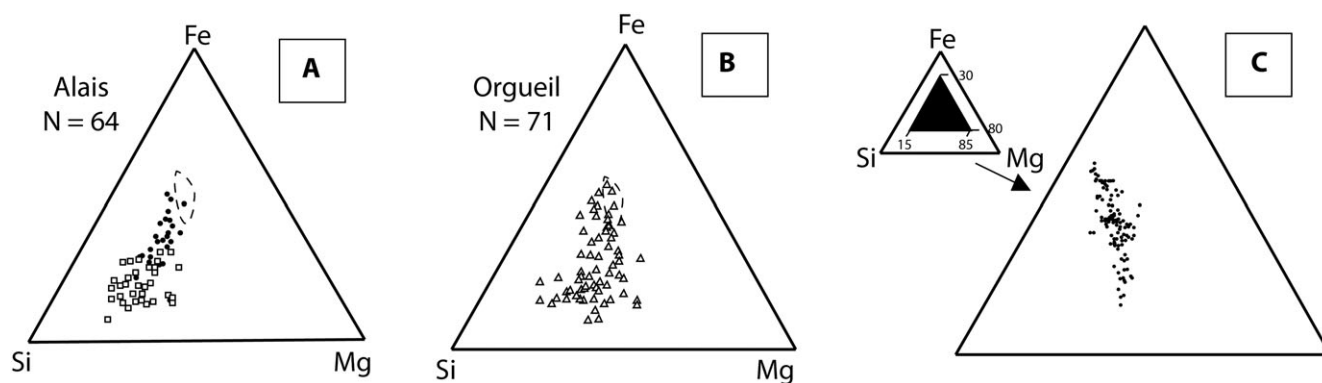


Fig. 2. Mg-Fe-Si diagrams showing the compositions of the very fine-grained layer silicate matrix compositions in the Alais (A) and Orgueil (B) meteorites (Mackinnon and Kaser 1988), and CI chondrite matrix compositions (C) (McSween 1987) including the bulk matrix compositions of the Tonk, Alais, Orgueil, and Ivuna CI meteorites (dots in c).

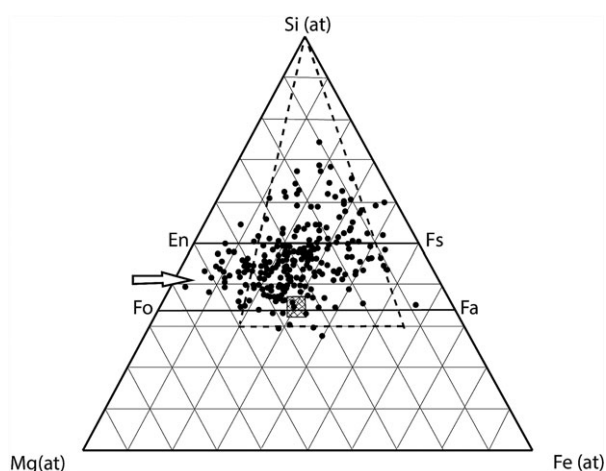


Fig. 3. GEMS compositions from a survey of 239 GEMS (Keller and Messenger 2011) (note the different orientation of this figure compared to Figs. 1 and 2). The trapezoid area delineates the range of GEMS compositions in CP IDP L2011K7. GEMS compositions overlap with the solar composition (hatched square). The triangle (dashed) show the range of Si- and Fe-rich GEMS from this survey (Keller and Messenger 2011). The arrow points to a field of very low Mg-Fe-Si GEMS that overlay the compositions of coarse-grained Mg-rich ferromagnesian silicate principal components in chondritic IDPs (Rietmeijer 2002).

(Rietmeijer and Nuth 2002; Rietmeijer et al. 2002). This work finds that highly vesicular GEMS are indirect evidence for water in comet Wild 2.

## EXPERIMENTAL PROCEDURES

Ultramicrotomed (70 nm) sections cut from allocation C2044,2,41,2,5 (track #41) were embedded in Embed812 epoxy and placed on a 10 nm thick amorphous carbon film supported on a standard Cu TEM grid at the NASA Johnson Space Center

STARDUST Curatorial Facility. This track was classified as a 4 mm turnip-shaped type B/C or C-type track made by a volatile-rich projectile (Hörz et al. 2006). All analyses were performed using a JEOL 2010 high-resolution transmission electron microscope (HRTEM) that operated at a 200 keV accelerating voltage and is capable of a 0.19 nm point to point resolution. This instrument is equipped with an Oxford INCA system with an ultra-thin window energy-dispersive X-ray detector capable of detecting all elements down to boron. The data were reduced using the standard Cliff-Lorimer thin film procedure at UNM. Focused analytical probe sizes (5, 10, or 15 nm) were selected to be smaller than an object-of-interest wherever possible but maintaining an optimum combination of the electron beam probe size and EDS acquisition time ensuring statistically relevant signal-to-noise ratios. Selecting an appropriate analytical spot size, I randomly probed numerous spots in post-flight silica aerogel and silica glass ranging from pure silica, pure MgO-bearing silica glass, and magnesian silica typically with numerous electron-opaque Fe-Ni-S nanograins. The chosen analytical spot size for analyses of electron-opaque inclusions >35 nm tends to have very little admixed glass. The EDS data for each embedded particle are accompanied by at least one EDS analysis of its surrounding silica aerogel or glass matrix, and in many instances more. The instrument is fitted with a GATAN Orius high-speed CCD camera for digital image acquisition.

The preflight silica aerogel contains ppm- and ppb-level impurity elements (Tsou et al. 2003) that may cause a chemical background (BKG) in silica glass. This background needs to be removed from the measured compositions which can be done by (1) discarding areas with “<1% of non-SiO<sub>2</sub>” (oxides) from further consideration (Stodolna et al. 2009), (2) ignoring SiO<sub>2</sub>

glass >99.5 mole% (Stodolna et al. 2012), and (3) using the differences in the measured element abundances in post-flight silica aerogel and in electron-opaque inclusion-free silica glass (Rietmeijer 2009b, 2009c, 2015). I prefer the third method that removed all Na and Cl from silica and magnesiosilica glass in this allocation.

## OBSERVATIONS

The overall low-Mg magnesiosilica glass with embedded Fe-Ni-S nanograins contains many round vesicles resembling those in vesicular glass allocation C5054,0,35,52,3 that probably arose inside boiling melted silica aerogel trapped during ultrafast quenching (Leroux 2012). There is likely to be a large range in temperatures involved in these kinds of interaction ranging from just melting and very viscous silica and to ultralow viscosity silica to actual vaporization. Thus, there is no predictable pattern of silica glass–Wild 2 dust interactions. This allocation contains several compact spherical magnesiosilica glass objects with embedded Fe-Ni-S grains (Fig. 4A) but they lack the tight GEMS morphology. A similar, but somewhat more organized, GEMS-like object is present in the silica glass matrix of allocation C2054,0,35,52,2 (Rietmeijer 2015). It may just be a matter of location within a Stardust track and impact temperature but GEMS-like objects are not an oddity. In this allocation though there are several highly vesicular objects of low-Mg magnesiosilica glass with embedded Fe-Ni-S nanograins (Fig. 4B). These vesicular objects probably formed within the expanding cavity of this turnip-shaped type B/C or type C track caused by volatile-rich projectile and probably very most close to the tile surface.

## PETROGRAPHIC CONTEXT

The glass matrix is a patchwork of different interactions between low-Mg magnesiosilica melts and Fe-Ni-S nanograins but with interspersed patches of mostly pure silica glass and very low-Mg magnesiosilica glass with trace amounts of Fe (0.2–4.2 atom%) and sulfur (0.2–3.2 atom%) due to scattered tiny Fe-S grains. Most silica-rich glass has a low-MgO magnesiosilica composition, viz. MgO =  $5.3 \pm 2.5$  wt% (range: 1.3–14.5;  $N = 89$ ). This DME (deep metastable eutectic) magnesiosilica composition indicates that this melt quenched rapidly (Rietmeijer et al. 2002), which is no surprise. A single outlier composition, MgO = 27.5 wt%, is close to the “enstatitic” eutectic composition in the MgO-SiO<sub>2</sub> phase diagram (Rietmeijer 2016a).

In other magnesiosilica glass patches, MgO =  $5.6 \pm 4.5$  (range: 1.5–19%) show a skewed normal distribution. Their 2.8% MgO modal value match the low-MgO eutectic point in the MgO-SiO<sub>2</sub> phase diagram (Ehlers 1972), which is a common, thermodynamically stable silica glass composition (Roskosz et al. 2008). Its presence suggests (local?) chemical equilibrium during hypervelocity capture. It has small patches of magnesiosilica glass, MgO =  $4.0 \pm 1.8$  wt% (range: 1.8–9.9 wt%;  $N = 21$ ), with tiny Fe-Ni-S grains (Ni = 0.2 atom%; range: 0.1–0.4). These patches contain Ca (average: 0.15 atom%) and sporadic Ca-spots (<0.4 atom%), as well as small Al-bearing domain (1.2–3.0 atom% Al) and a few Cr-spots (<1.2 atom%). A single 5 nm electron-opaque grain has a stoichiometric daubréelite.

The Mg-Fe-S (atom%) compositions (Fig. 5A) do not show the “familiar” patterns (e.g., Leroux 2012; Stodolna et al. 2012) but instead show a very low-Mg ferromagnesiosilica glass distribution (Rietmeijer 2015). This mixing pattern, and its extent of mixing Mg-silicates and Fe(Ni)-sulfides, is entirely determined in the latter and a dearth of assimilated Mg-rich olivine and/or Mg-rich pyroxene during hypervelocity capture. There are also many surviving fragments of Fe-Ni-S (69%), Ni-free Fe<sub>2</sub>S (29%), and Fe(±Ni) grains (2%) ranging in size from 5 nm to 102.5 nm. They are mostly Ni-free and low-Ni pyrrhotite (Fig. 5B). The mean grain size is  $28.2 \pm 20.3$  nm size ( $N = 100$ ; range: 5–102.5 nm; modal value: 17 nm). The largest grain, 120 nm × 85 nm, is a low-Ni sulfide.

## DISCUSSION AND CONCLUSIONS

Allocation C2044,2,41,2,5 is a simple mixture of Fe-Ni-S sulfides and magnesiosilica glass in pure silica generated during hypervelocity capture when forsterite and/or enstatite fragments interacted with silica melts inside an expanding cavity of the developing track (Trigo-Rodríguez et al. 2008). This allocation captured the interactions at the very moment of impact of a volatile-rich projectile. There is no evidence of vapor-condensed magnesiosilica grains (Rietmeijer et al. 2002; Rietmeijer and Nuth 2015). The overall low magnesiosilica glasses are (1) low-Mg silica glass with a low-MgO eutectic equilibrium composition of 1715 °C and (2) high-MgO magnesiosilica glass with deep metastable eutectic compositions due to ultrafast quenching of an MgO-SiO<sub>2</sub> liquid at >2000 °C. The smallest Fe-Ni-S fragments assimilated in the silica and magnesiosilica melts. The mostly >10 nm Fe-Ni-S, Ni-free Fe<sub>2</sub>S and Fe(±Ni) fragments were assimilated in vesicular magnesiosilica glasses resembling vesicular silica-rich glass thought to be due local boiling of silica aerogel at high temperatures (b.p. 2230 °C) (Leroux 2012).

The vast majority of GEMS, >95% (Keller and Messenger 2011), are solar system grains that were available for accretion into developing asteroids and

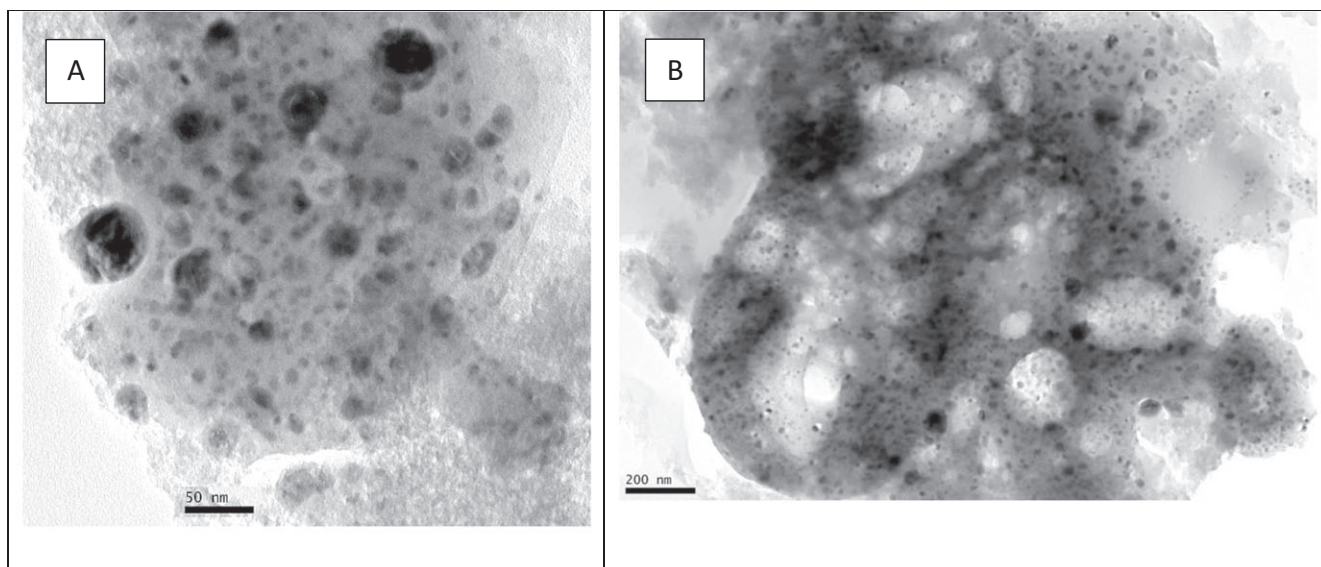


Fig. 4. TEM images of (A) a spherical magnesiosilica glass blob with randomly embedded small Fe-Ni-S grains and (B) a highly vesicular object of magnesiosilica glass with numerous small Fe-Ni-S nanograins in allocation C2044,2,41,2,5. There is a small area of pure silica glass with a narrow rim of Fe-Ni-S nanograins (upper right-hand corner).

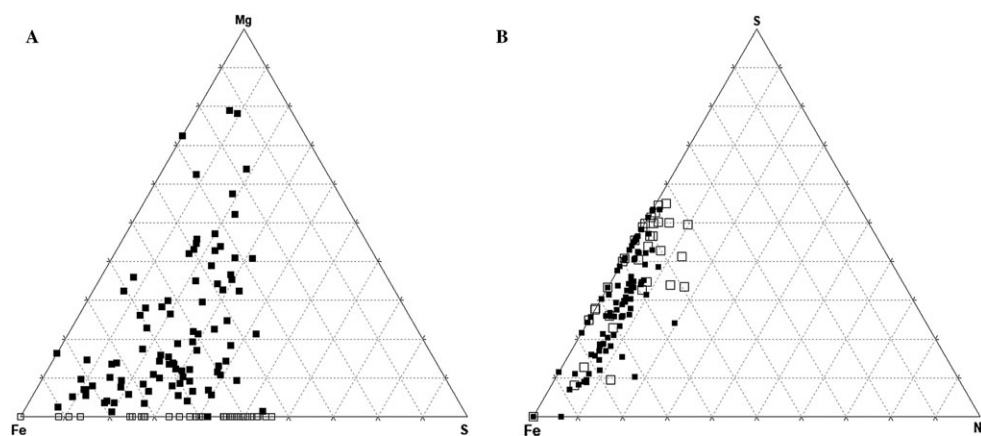


Fig. 5. A) Mg-Fe-S (atom%) compositions in low-MgO glass in allocation C2044,2,41,2,5 (solid squares) and Fe(Ni)-S nanograins (open squares) in very low-Mg magnesiosilica glass and (B) Fe-Ni-S (atom%) compositions of 100 Fe-Ni-S grains in pure silica and magnesiosilica glasses.

comet nuclei. So far, no bona fide GEMS were identified in comet Wild 2, only GEMS-like objects (Zolensky et al. 2006; Stodolna et al. 2012; Leroux and Jacob 2013; Rietmeijer 2015). These objects though appear to be “accidental Fe-Ni-S grain concentrations within a glass globule” (Fig. 4A) that moved freely through silica-rich melt during hypervelocity capture. It is noted that this does not necessarily disqualify them as captured GEMS.

The most spectacular features in this allocation are the rare, highly, vesicular GEMS-glass bubbles. This is not entirely unexpected as this allocation was a type B/

C or C-type track made by a volatile-rich projectile that contained some amount of water. So far evidence of hydrous phases has proved elusive among the Stardust samples albeit that layer silicates, and other OH-bearing rich phases might still be found along the walls of bulbous tracks or at track termini (Zolensky et al. 2008) but no such phases have been reported. Hypervelocity ( $\sim 6.2 \text{ km s}^{-1}$ ) impact experiments using serpentine, cronstedtite, and Muchison meteorite targets with an average  $10 \mu\text{m}$  to  $30 \mu\text{m}$  grain size caused significant near-surface vesiculation, amorphization, and melting (Noguchi et al. 2007). While these experiments showed

that hypervelocity impact capture induces vesiculation, and probably also causes volatile loss, the experiments do not exactly replicate the response for much smaller Wild 2 grains. Brownlee et al. (2006) submitted that “if abundant hydrated silicates >200 nm existed in Wild 2, there should be clear evidence of them in the analyzed samples.” There is none, but ~200 nm anhydrous Ca,K-aluminosilica and Mg-rich olivine grains survived (Rietmeijer 2016b).

What could be the source, or sources, of water in comet Wild 2? The answer lies in large-scale radial mixing during the accretion phase in the solar nebula from debris from the inner nebula to the Kuiper Belt (Brownlee et al. 2006). There is ample evidence for widespread aqueous alteration in the early solar system in the form of surviving partially and fully hydrated GEMS and CI meteorites that formed “dirty snowballs.” These objects of 3 Myr old material from the inner solar system were incorporated into comet nuclei (Davidsson et al. 2016).

I submit that GEMS, partially hydrated GEMS, and fully hydrated GEMS in the early solar system accreted into small dirty-ice balls of CP IDPs, and up to objects that are the surviving CI meteorites. The argument rests on the fact that CI meteorites and (partially) hydrated GEMS in chondritic IDPs have identical compositions and mineralogy dominated by serpentine and/or montmorillonite. It is almost certain that Jupiter-family comet 81P/Wild 2 contained water in hydrated GEMS. This work submits that highly vesicular GEMS-glass in Stardust samples are evidence that water was present in the Wild 2 nucleus from hydrated GEMS.

*Acknowledgments*—This work was supported by NASA LARS grant NNX14AF21G (FJMR). Transmission electron microscope analyses were carried out in the Electron Microbeam Analysis Facility of the Department of Earth and Planetary Sciences at the University of New Mexico. I thank Don Brownlee for constructive inputs during the review process.

*Editorial Handling*—Dr. Donald Brownlee

## REFERENCES

- Bradley J. P. 1994a. Chemically anomalous, pre-accretionally irradiated grains in interplanetary dust from comets. *Science* 265:925–929.
- Bradley J. P. 1994b. Nanometer-scale mineralogy and petrography of fine-grained aggregates in anhydrous interplanetary dust particles. *Geochimica et Cosmochimica Acta* 58:2123–2134.
- Bradley J. P., Germani M. S., and Brownlee D. E. 1989. Automated thin-film analyses of anhydrous interplanetary dust particles in the analytical electron microscope. *Earth and Planetary Science Letters* 93:1–13.
- Brownlee D., Tsou P., Aléon J., Alexander C. M. O'D., Araki T., Bajt S., Baratta G. A., Bastien R., Bland Ph., Bleuet P., Borg J., Bradley J. P., Brearley A., Brenker F., Brennan S., Bridges J. C., Browning N. D., Brucato J. R., Bullock E., Burchell M. J., Busemann H., Butterworth A., Chaussidon M., Chevront A., Chi M., Cintala M. J., Clark B. C., Clemett S. J., Cody G., Colangeli L., Cooper G., Cordier P., Daghlian C., Dai Z., D'Hendecourt L., Djouadi Z., Dominguez G., Duxbury T., Dworkin J. P., Ebel D. S., Economou T. E., Fakra S., Fairey S. A. J., Fallon S., Ferrini G., Ferroir T., Fleckenstein H., Floss C., Flynn G., Franchi I. A., Fries M., Gainsforth Z., Gallien J.-P., Genge M., Gilles M. K., Gillet P., Gilmour J., Glavin D. P., Gounelle M., Grady M. M., Graham G. A., Grant P. G., Green S. F., Grossemy F., Grossman L., Grossman J. N., Guan Y., Hagiya H., Harvey R., Heck P., Herzog G. F., Hoppe P., Hörz F., Huth J., Hutcheon I. D., Ignatyev K., Ishii H., Ito M., Jacob D., Jacobsen C., Jacobsen S., Jones S., Joswiak D., Jurewicz A., Kearsley A. T., Keller L. P., Khodja H., Kilcoyne A. L. D., Kissel J., Krot A., Langenhorst F., Lanzirrotti A., Le L., Leshin L. A., Leitner J., Lemelle L., Leroux H., Liu M.-C., Luening K., Lyon I., MacPherson G., Marcus M. A., Marhas K., Marty B., Matrajt G., McKeegan K., Meibom A., Mennella V., Messenger K., Messenger S., Mikouchi T., Mostefaoui S., Nakamura T., Nakano T., Newville M., Nittler L. R., Ohnishi I., Ohsumi K., Okudaira K., Papanastassiou D. A., Palma R., Palumbo M. E., Pepin R. O., Perkins D., Perronnet M., Pianetta P., Rao W., Rietmeijer F. J. M., Robert F., Rost D., Rotundi A., Ryan R., Sandford S. A., Schwandt G. S., See T. H., Schlutter D., Sheffield-Parker J., Simionovici A., Simon S., Sitnitsky I., Snead C. J., Spencer M. K., Stadermann F., Steele A., Stephan T., Stroud R., Susini J., Sutton S. R., Suzuki Y., Taheri M., Taylor S., Teslich N., Tomeoka K., Tomioka N., Toppani A., Trigo-Rodríguez J. M., Troadec D., Tsuchiyama A., Tuzzolino A. J., Tylliszczak T., Uesugi K., Velbel M., Vellenga J., Vicenzi E., Vincze L., Warren J., Weber I., Weisberg M., Westphal A. J., Wirick S., Wooden D., Wopenka B., Wozniakiewicz P., Wright I., Yabuta H., Yano H., Young E. D., Zare R. N., Zega T., Ziegler K., Zimmerman L., Zinner E., and Zolensky M. 2006. Comet 81P/Wild 2 under a microscope. *Science* 314:1711–1716.
- Chi M., Ishii H., Dai Z. R., Toppani A., Joswiak D. J., Leroux H., Zolensky M., Keller L. P., Browning N. D., and Bradley J. P. 2007. Does Comet Wild-2 contain GEMS? (abstract #2010). 38th Lunar and Planetary Science Conference. CD-ROM.
- Davidsson B. J. R., Sierks H., Güttler C., Marzari F., Pajola M., Rickman H., A'Hearn M. F., Auger A.-T., El-Maarry M. R., Fornasier S., Gutiérrez P. J., Keller H. U., Massironi M., Snodgrass C., Vincent J.-B., Barbieri C., Lamy P. L., Rodrigo R., Koschny D., Barucci M. A., Bertaux J.-L., Bertini I., Cremonese G., Da Deppo V., Debei S., De Cecco M., Feller C., Fulle M., Groussin O., Hviid S. F., Höfner S., Ip W.-H., Jorda L., Knollenberg J., Kovacs G., Kramm J.-R., Kürt E., Küppers M., La Forgia F., Lara L. M., Lazzarin M., Lopez Moreno J. J., Moissl-Fraund R., Mottola S., Naletto G., Oklay N., Thomas N., and Tubiana C. 2016. The primordial nucleus of comet 67P/Churyumov-Gerasimenko. *Astronomy &*

- Astrophysics* 592: A63. <https://doi.org/10.1051/0004-6361/201526968>
- Ehlers E. G. 1972. *The interpretation of geological phase diagrams*. San Francisco, California: W. H. Freeman and Company. 280 p.
- Hicks L. J., MacArthur J. L., Bridges J. C., Price M. C., Wickham-Eade J. E., Burchell M. J., Hansford G. M., Butterworth A. L., Gurman S. J., and Baker S. H. 2017. Magnetite in Comet Wild 2: Evidence for parent body aqueous alteration. *Meteoritics & Planetary Science* 52:2075–2096. <https://doi.org/10.1111/maps.12909>.
- Hörz F., Bastien R., Borg J., Bradley J. P., Bridges J. C., Brownlee D. E., Burchell M. J., Chi M., Cintala M. J., Dai Z. R., Djouadi Z., Dominguez G., Economou T. E., Fairey S. A. J., Floss C., Franchi I. A., Graham G. A., Green S. F., Heck P., Hoppe P., Huth J., Ishii H., Kearsley A. T., Kissel J., Leitner J., Leroux H., Marhas K., Messenger K., Schwandt C. S., See T. H., Snead C., Stadermann F. J., Stephan T., Stroud R., Teslich N., Trigo-Rodríguez J. M., Tuzzolino A. J., Troadec D., Tsou P., Warren J., Westphal A., Wozniakiewicz P., Wright I., and Zinner E. 2006. Impact features on Stardust: Implications for comet 81P/Wild 2 dust. *Science* 314:1716–1719.
- Joswiak D. J., Brownlee D. E., Bradley J. P., Schlutter D. J., and Pepin R. O. 1996. Systematic analyses of major element distributions in GEMS from high speed IDPs. Proceedings, 27th Lunar and Planetary Science Conference. pp. 625–626.
- Joswiak D. J., Brownlee D. E., Matrajt G., Westphal A. J., Snead C. J., and Gainsforth Z. 2012. Comprehensive examination of large mineral and rock fragments in Stardust tracks: Mineralogy, analogous extraterrestrial materials, and source regions. *Meteoritics & Planetary Science* 47:471–524.
- Keller L. P. and Messenger S. 2011. On the origins of GEMS grains. *Geochimica et Cosmochimica Acta* 75:5336–5365.
- Leroux H. 2012. Fine-grained material of 81P/Wild 2 in interaction with Stardust aerogel. *Meteoritics & Planetary Science* 47:613–622.
- Leroux H. and Jacob D. 2013. Fine-grained material encased in microtracks of Stardust samples. *Meteoritics & Planetary Science* 48:1607–1617.
- Mackinnon I. D. R. and Kaser S. A. 1988. The clay-size fraction of CI chondrites Alais and Orgueil: An AEM study. Proceedings, 19th Lunar and Planetary Science Conference. pp. 709–710.
- McSween H. Y. Jr. 1987. Aqueous alteration in carbonaceous chondrites: Mass balance constraints on matrix mineralogy. *Geochimica et Cosmochimica Acta* 51:2469–2477.
- Noguchi T., Nakamura T., Okudaira K., Yano H., Sugita S., and Burchell M. J. 2007. Thermal alteration of hydrated minerals during hypervelocity capture to silica aerogel at the flyby speed of Stardust. *Meteoritics & Planetary Science* 42:357–72.
- Rietmeijer F. J. M. 1993. Size distributions in two porous chondritic micrometeorites. *Earth and Planetary Science Letters* 117:609–617.
- Rietmeijer F. J. M. 1996. The butterflies of principal components: A case of ultrafine-grained polyphase units. Proceedings, 27th Lunar and Planetary Science Conference. pp. 1073–1074.
- Rietmeijer F. J. M. 1998. Interplanetary dust particles. In *Planetary materials*, edited by Papike J. J. Reviews in Mineralogy, vol. 36. Chantilly, Virginia: Mineralogical Society of America. pp. 2-1–2-95.
- Rietmeijer F. J. M. 2002. The earliest chemical dust evolution in the solar nebula. *Chemie der Erde Geochemistry* 62:1–45.
- Rietmeijer F. J. M. 2009a. A cometary aggregate interplanetary dust particle as an analog for comet Wild 2 grain chemistry preserved in silica-rich Stardust glass. *Meteoritics & Planetary Science* 44:1589–1609.
- Rietmeijer F. J. M. 2009b. Stardust glass: Indigenous and modified comet Wild 2 particles. *Meteoritics & Planetary Science* 44:1707–1715.
- Rietmeijer F. J. M. 2009c. Chemical identification of comet 81P/Wild 2 dust after interacting with molten silica aerogel. *Meteoritics & Planetary Science* 44:1121–1132.
- Rietmeijer F. J. M. 2011. Pre-accretionary and parent body histories of a cometary aggregate particle. *Icarus* 211:948–959.
- Rietmeijer F. J. M. 2015. The smallest comet 81P/Wild 2 dust dances around the CI composition. *Meteoritics & Planetary Science* 50:1767–1789. <https://doi.org/10.1111/maps.12510>.
- Rietmeijer F. J. M. 2016a. At the interface of silica glass and compressed silica aerogel in Stardust track 10: Comet Wild 2 is not a goldmine. *Meteoritics & Planetary Science* 51:574–583. <https://doi.org/10.1111/maps.12608>.
- Rietmeijer F. J. M. 2016b. Energy dissipation at the silica glass/compressed aerogel interface: The fate of Wild 2 mineral grains and fragments smaller than ~100 nm. *Meteoritics & Planetary Science* 51:1871–1885. <https://doi.org/10.1111/maps.12695>.
- Rietmeijer F. J. M. and Nuth J. A. III. 2002. Experimental astromineralogy: Circumstellar ferromagnesian dust in analogs and natural samples. In *Dust in the solar system and other planetary systems, COSPAR Colloquia Series, 15*, edited by Green S. F., Williams I. P., McDonnell J. A. M. and McBride N. Amsterdam, the Netherlands: Pergamon Elsevier Science. pp. 333–339.
- Rietmeijer F. J. M. and Nuth J. A. III. 2015. Gas-phase condensation experiments of magnesium iron silicates. In *Laboratory modern astrochemistry, from molecules through nanoparticles to grains*, edited by Schlemmer S., Giessen T., Mutschke H. and Jäger C. Weinheim, Germany: Wiley-VCH Verlag GmbH & Co. KGaA. pp. 455–466.
- Rietmeijer F. J. M., Nuth J. A. III, Karner J. M., and Hallenbeck S. L. 2002. Gas to solid condensation in a Mg-SiO<sub>2</sub>-H<sub>2</sub>-O<sub>2</sub> vapor: Metastable eutectics in the MgO-SiO<sub>2</sub> phase diagram. *Physical Chemistry Chemical Physics* 4:546–551.
- Rietmeijer F. J. M., Nuth J. A. III, and Pun A. 2013. The formation of Mg, Fe-silicates by reactions between amorphous magnesian silica smoke particles and metallic iron nanograins with implications for comet silicate origins. *Meteoritics & Planetary Science* 48:1823–1840. <https://doi.org/10.1111/maps.12194>.
- Roskosz M., Leroux H., and Watson H. C. 2008. Thermal history, partial preservation and sampling bias recorded by Stardust cometary grains during their capture. *Earth and Planetary Science Letters* 273:195–202.
- Sandford S. A. and Walker R. M. 1985. Laboratory infrared transmission spectra of individual interplanetary dust particles from 2.5 to 25 microns. *The Astrophysical Journal* 291:838–851.

- Stodolna J., Jacob D., and Leroux H. 2009. A TEM study of four particles extracted from the Stardust track 80. *Meteoritics & Planetary Science* 44:1511–1518.
- Stodolna J., Jacob D., and Leroux H. 2012. Mineralogy and petrology of Stardust particles encased in the bulb of track 80: TEM investigation of the Wild 2 fine-grained material. *Geochimica et Cosmochimica Acta* 87:35–50.
- Tomeoka K. and Buseck P. R. 1985. Hydrated interplanetary dust particle linked with carbonaceous chondrites? *Nature* 314:338–340.
- Trigo-Rodríguez J. M., Domínguez G., Burchell M. J., Hörz F., and Llorca J. 2008. Bulbous tracks arising from hypervelocity capture in aerogel. *Meteoritics & Planetary Science* 43:75–86.
- Tsou P., Brownlee D. E., Hörz F., Sandford S. A., and Zolensky M. E. 2003. Wild 2 and interstellar sample collection and Earth return. *Journal of Geophysical Research* 108:E8113.
- Zolensky M. E. and Thomas K. L. 1995. Iron- and iron-nickel sulfides in chondritic interplanetary dust particles. *Geochimica et Cosmochimica Acta* 59:4707–4712.
- Zolensky M. E., Zega T. J., Yano H., Wirick S., Westphal A. J., Weisberg M. K., Weber I., Warren J. L., Velbel M. A., Tsuchiyama A., Tsou P., Toppani A., Tomioka N., Tomeoka K., Teslich N., Taheri M., Susini J., Stroud R., Stephan T., Stadermann F. J., Snead C. J., Simon S. B., Simionovici A., See T. J., Robert F., Rietmeijer F. J. M., Rao W., Perronnet M. C., Papanastassiou D. A., Okudaira K., Ohsumi K., Ohnishi I., Nakamura-Messenger K., Nakamura T., Mostefaoui S., Mikouchi T., Meibom A., Matrajt G., Marcus M. A., Leroux H., Lemelle L., Le L., Lanzirotti A., Langenhorst F., Krot A. N., Keller L. P., Kearsley A. T., Joswiak D., Jacob D., Ishii H., Harvey R., Hagiya K., Grossman L., Grossman J. N., Graham G. A., Gounelle M., Gillet P., Genge M. J., Flynn G., Ferroir T., Fallon S., Ebel D. S., Dai Z., Cordier P., Clark B., Chi M., Butterworth A. L., Brownlee D. E., Bridges J. C., Brennan S., Brearley A., Bradley J. P., Bleuet P., Bland P. A., and Bastien R. 2006. Mineralogy and petrology of comet Wild 2 nucleus samples. *Science* 314:1735–1739.
- Zolensky M., Nakamura-Messenger K., Sverdrup J., Rietmeijer F., Leroux H., Mikouchi T., Ohsumi K., Simon S., Grossman L., Stephan T., Weisberg M., Velbel M., Zega T., Stroud R., Tomeoka K., Ohnishi I., Tomioka N., Nakamura T., Matrajt G., Joswiak J., Brownlee D., Langenhorst F., Krot A., Kearsley A., Ishii H., Graham G., Dai Z. R., Chi M., Bradley J., Hagiya K., Gounelle M., and Bridges J. 2008. Comparing Wild 2 particles to chondrites and IDPs. *Meteoritics & Planetary Science* 43:261–272.
-